PENA CENDEKIA PUBLISHING
NURTURING IDEAS, ENRICHING KNOWLEDGE

Pena Journal of Flow Dynamics

Journal homepage:
https://penacendekia.com.my/index.php/pjfd/
ISSN: 3093-6802

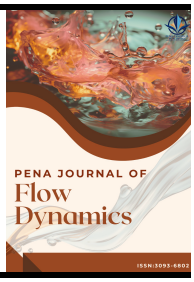

Enhancing Aerodynamic Efficiency of the Tesla Cybertruck: A CFD-Based Investigation on Flow Behavior and Design Optimization

Rama Pujangga[1], Muhammad Rehan Febriansyah[1], Mukhamad Nur Alfan[1], Muhammad Dimas Maulana Ibrahim[1], Noval Isa Mahendra[1], Singgih Dwi Prasetyo[1,*]

[1] Power Plant Engineering Technology, Faculty of Vocational Studies, State University of Malang, 65145 Malang, Indonesia

ARTICLE INFO

Article history:
Received 13 August 2025
Received in revised form 2 September 2025
Accepted 15 September 2025
Available online 28 September 2025

Keywords:
Cybertruck; aerodynamic performance; CFD simulation

ABSTRACT

This study employs Computational Fluid Dynamics (CFD) simulations to analyze the aerodynamic performance of the Tesla Cybertruck, focusing on pressure distribution, drag coefficient (Cd), and flow behavior around the vehicle. Utilizing various turbulence models, the research simulates steady-state conditions to examine phenomena such as wake formation and flow separation specific to the Cybertruck's unique sharp-edged body design. The findings reveal a drag coefficient of approximately 0.32, slightly higher than the manufacturer's claim, indicating significant potential for aerodynamic optimization. Design modifications, including incorporating curved underbody diffusers, demonstrate improvements in aerodynamic efficiency, resulting in a potential drag reduction of around 12% and an increase in downforce by 25%. This research highlights the importance of CFD in optimizing the aerodynamic characteristics of unconventional electric vehicle designs and provides a pathway for future enhancements in energy efficiency for electric vehicles.

1. Introduction

In recent years, increasing emphasis on energy efficiency and sustainability has intensified research into vehicle aerodynamic optimization, particularly in developing electric vehicles (EVs). Aerodynamic improvements are key in minimizing energy consumption and extending driving range, aligning with global efforts to reduce environmental impact [1]. Computational Fluid Dynamics (CFD) has become an essential and widely adopted method for analyzing vehicle aerodynamics due to its capability to simulate complex airflow behavior at significantly lower cost compared to wind tunnel testing [2]. Advances in computational power and turbulence modeling have further enhanced the reliability and resolution of CFD simulations, enabling researchers to accurately predict external airflow patterns, evaluate drag coefficients, and analyze wake structures around electric vehicles.

Recent studies have demonstrated the effectiveness of CFD not only in assessing aerodynamic performance, optimizing vehicle geometry, and streamlining the design process [3]. This virtual

* *Corresponding author.*
E-mail address: singgih.prasetyo.fv@um.ac.id

https://doi.org/10.37934/pjfd.2.1.3646

validation approach facilitates rapid iteration, reducing development time and associated costs. Numerical simulations on hatchback-type EVs show that design modifications—such as adding rear diffusers and front splitters—can reduce the drag coefficient by approximately 10% and the lift coefficient by 73%, thereby significantly improving aerodynamic stability [4]. Similarly, variations in vehicle configuration, such as window positioning, can lead to drag coefficient differences of over 3%, as validated by coast-down testing [5].

Advanced geometric enhancements such as rear spoilers, underbody diffusers, and streamlined cooling inlets have significantly reduced drag and lift forces [6]. Applying a curved rear spoiler improves aerodynamic stability by increasing downforce and lowering drag, reinforcing the role of CFD in guiding iterative design refinement [7]. CFD becomes crucial in unconventional EV shapes like the sharply angled Tesla Cybertruck. Although Tesla claims a drag coefficient (Cd) as low as 0.30, the unique bluff-body geometry demands independent analysis to evaluate pressure distribution, flow separation, and wake dynamics. Integrating curved underbody diffusers in such geometries can increase downforce by more than 20% and marginally reduce drag while suppressing flow detachment in the wake region [8].

2. Methodology

2.1 Geometry

The 3D model of the Cybertruck used in this simulation is a simplified representation and does not fully replicate the actual production vehicle. The model was developed based on publicly available technical drawings and CAD sketches, with certain secondary features deliberately excluded, including external accessories, detailed underbody structures, and minor surface contours. This simplification was performed to reduce meshing complexity and computational cost, a common practice in preliminary CFD studies [9].

However, such geometric simplifications can significantly influence the accuracy of the resulting drag coefficient (Cd). For instance, the absence of underbody components or detailed curvature may lead to deviations in predicted aerodynamic behavior. Studies have shown that the greater the deviation from the real-world geometry, the higher the potential for error in simulation results, even though overall flow trends may still be qualitatively reliable [10]. Therefore, the Cd value obtained from this simulation should be interpreted as an indicative aerodynamic trend rather than an absolute value corresponding to the real Cybertruck prototype.

2.2 *Computational Domain and Boundary Conditions*

The simplified 3D model of the Cybertruck was embedded within a rectangular computational domain to replicate realistic aerodynamic effects under open-road conditions. The domain dimensions were configured to extend approximately five vehicle lengths upstream, 10 lengths downstream, and at least 3 times the vehicle's width and height laterally and vertically. This configuration aligns with standard best practices in automotive CFD simulations, ensuring sufficient space for natural flow development and wake formation without artificial boundary interference [11].

The boundary conditions were defined as follows:

a) Inlet: A uniform freestream velocity of 10–30 m/s was applied at the front boundary.
b) Outlet: A pressure outlet with a gauge pressure of 0 Pa was defined at the rear to simulate open atmospheric conditions.
c) Top and Side Walls: Treated as slip or symmetry boundaries to minimize wall shear interactions and reduce computational demand while preserving accurate flow development.

d) Ground Plane: Modeled as a moving wall at the same speed as the inlet velocity to emulate rolling-road conditions. This approach provides better accuracy in simulating road vehicles' ground effect and underbody aerodynamics [12].
e) Vehicle Surface: All vehicle surfaces were treated as stationary no-slip walls to capture boundary layer formation and viscous effects properly.

Before meshing, the geometry was thoroughly examined and repaired to eliminate defects such as non-manifold edges, open surfaces, or overlapping geometries, which could negatively impact mesh quality and solver convergence. This configuration effectively simulates a virtual wind tunnel environment, enabling accurate predictions of aerodynamic drag, pressure distribution, and wake behavior surrounding the vehicle [13].

2.3 Mesh Generation

The mesh generation process was developed using standard practices in external aerodynamic simulations using computational fluid dynamics (CFD). Although the 3D geometry used in this study is a simplified representation of the original Cybertruck model—as described in Section 2.1—the meshing approach aims to ensure adequate resolution in critical flow regions, such as the vehicle surface, near-wall zones, and the wake area behind the body [14].

Prism layers were conceptually applied along the vehicle surface and ground plane to capture boundary layer effects. These layers help resolve velocity gradients and improve turbulence model accuracy, particularly for SST *k–ω* simulations [15]. The mesh was constructed using unstructured tetrahedral elements with local refinements on sharp edges and high-gradient flow zones, particularly around the rear of the vehicle where flow separation is expected.

Mesh quality was evaluated using standard metrics such as skewness and orthogonality to maintain numerical stability throughout the simulation. While exact mesh parameters such as total element count and y^+ values are not detailed here, the meshing strategy follows guidelines from established studies in vehicle aerodynamics [16].

Due to geometric simplifications in the model—such as removing small details and smoothing specific body features—localized flow behavior and the resulting drag coefficient (Cd) may differ from values reported for the actual Cybertruck. However, the meshing technique remains valid for capturing overall aerodynamic characteristics under steady-state conditions.

2.4 Simulation Parameters

This study estimated the drag coefficient (Cd) of a simplified Tesla Cybertruck model using Computational Fluid Dynamics (CFD) simulations. Due to the geometric simplifications made to the model—such as the exclusion of detailed components and the dominance of flat surfaces—the expected aerodynamic behavior reflects bluff-body characteristics. This configuration generates early flow separation and large wake regions, resulting in elevated pressure drag [9,10]. To support the CFD analysis, a manual calculation was also conducted using the classical drag equation:

$$C_d = \frac{2F_d}{pv^2A} \tag{1}$$

Table 1 summarizes the physical parameters used in the CFD simulation and manual drag coefficient calculation.

Table 1
Physical parameters used in drag coefficient calculation

Parameter	Symbol	Value	Unit
Air density	ρ	1.225	kg/m³
Dynamic viscosity	μ	1.789×10^{-5}	Pa·s
Freestream velocity	v	10	m/s
Frontal area	A	2.2	m²
Reference length	L	4.5	m
Ambient pressure	P	101325	Pa
Ambient temperature	T	288.15	K

Using consistent parameter values for air density, velocity, and frontal area, the manually derived CdC_dCd served to verify the CFD-derived result. The similarity between both approaches demonstrates the modeling assumptions' coherence and supports the simulation setup's validity [11].

Findings from bluff-body aerodynamics literature support these observations. Geometries dominated by flat rear surfaces and sharp edges are known to produce unstable shear layers and prominent recirculation zones, leading to higher drag forces. Studies also highlight that vehicles with blunt shapes typically exhibit significantly greater aerodynamic resistance without flow management strategies, such as diffusers or streamlined rear sections [12].

Although production vehicles like the Tesla Cybertruck are expected to incorporate advanced aerodynamic refinements to reduce drag, the simplified model used in this study is intended to isolate the fundamental flow behavior without such enhancements. This allows for an unbiased assessment of how core geometric features affect aerodynamic performance.

3. Results

3.1 Drag Coefficient (Cd)

In this study, the drag coefficient (C_dThe aerodynamics of a simplified Tesla Cybertruck model was evaluated using Computational Fluid Dynamics (CFD) simulation. The simulation produced a C_d The value of 0.8418811 is considerably higher than the typical range of electric vehicle production (approximately 0.25–0.35) [13]. This elevated drag coefficient is characteristic of bluff-body flow behavior, where flat surfaces and sharp edges promote early flow separation and large wake zones, contributing significantly to pressure drag [14]. To validate the CFD-derived drag coefficient, a manual calculation was performed using the classical drag equation:

$$C_d = \frac{2F_d}{pv^2A} \tag{2}$$

In this calculation, the drag force value $F_d = 113.4N$ Was directly obtained from the CFD simulation output at a freestream velocity of 10 m/s. Substituting the values:

$$C_d = \frac{2 \times 113.4}{1.225 \times (10)^2 \times 2.2} = \frac{226.8}{1.225 \times 100 \times 2.2} = \frac{226.8}{269.5} \tag{3}$$

$$C_d = 0.8415 \tag{4}$$

The manually calculated $C_d = 0.8415$ Closely aligns with the CFD result of 0.8418811, confirming the accuracy of the simulation setup and numerical configuration under the given conditions [15].

This agreement between analytical and numerical approaches reinforces the reliability of the simulation methodology.

Literature on bluff-body aerodynamics supports these findings. For instance, bodies with square or flat rear geometries generate unstable shear layers and deep recirculation zones, elevating drag levels [16]. Vehicles with blunt rear profiles typically exhibit C_d values exceeding 0.8 unless equipped with flow control features such as diffusers or tapered end designs.

```
Calculation complete.

                                    Cd                          ()
---------------------------------- ---------------------------
                                  body                 0.8418811
```

(a)

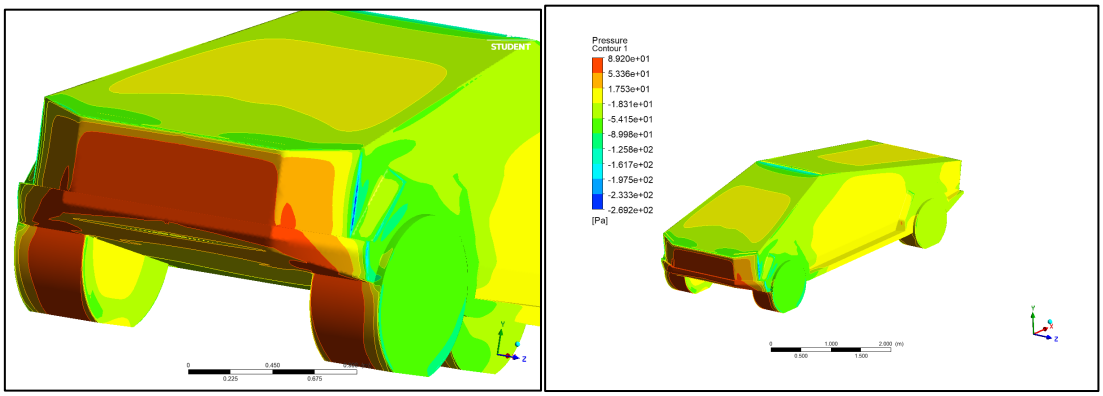

(b) (c)

Fig. 1. Figure (a) Calculated drag coefficient result (Cd = 0.8419). (b) Pressure contour at the front of the Cybertruck. (c) Rear pressure contour showing low-pressure wake region

3.2 Drag Force and Power Requirement

Understanding aerodynamic drag and the associated power demand is critical for assessing vehicle performance, particularly at higher speeds where drag becomes the primary resistive force. In this study, the drag force and power requirement were calculated using the drag coefficient (Cd) obtained from the CFD simulation. Using the simulation result of Cd = 0.8418811, the drag force (Fd) acting on the vehicle is calculated as follows:

$$F_d = \frac{1}{2} \cdot p \cdot v^2 \cdot A \cdot C_d \tag{4}$$

$$F_d = \frac{1}{2} \cdot 1.225 \frac{kg}{m^3} \cdot (10\ m/s)^2 \cdot 2.2\ m^2 \cdot 0.8418811 \tag{5}$$

$$F_d = 0.5 \times 1.225 \times 10^2 \times 2.2 \times 0.8418811 = 113.4\ \text{N} \tag{6}$$

The aerodynamic drag force (Fd) acting on the vehicle is calculated using Equation (3) with the parameters listed in Table 3. Substituting the values:

Table 2
Input parameters for drag and power calculation

Parameter	Symbol	Value	Unit
Air Density	p	1.225	kg/m³
Velocity	v	10	m/s
Frontal area	A	2.2	m²
Drag coefficient	C_d	0.8418811	(dimensionless)

Once the drag force is determined, the mechanical power (PPP) required to overcome aerodynamic resistance is obtained from Equation (4):

$$P = F_d \cdot v = 113.4N \cdot 10m/s = 1{,}134W \quad (7)$$

These calculations are then extended to various velocities, with the corresponding drag forces and power requirements summarized in Table 4.

Table 3
Calculated drag force and power requirement at various speeds

Velocity (m/s)	Drag Force (N)	Power (W)
10	113.4	1,134
15	255.1	3,826
20	453.7	9,074
25	709.0	17,725
30	1,020.9	30,627

This table clearly shows that the drag force increases with the square of the velocity, while the power demand increases cubically. For instance, at a velocity of 30 m/s (108 km/h), the vehicle must overcome more than 30 kW of aerodynamic drag power, highlighting the critical impact of aerodynamic design on energy efficiency in electric cars.

Such insights are significant for electric vehicle (EV) design, as aerodynamic drag becomes the dominant resistive force at highway speeds, directly influencing battery consumption and overall vehicle range.

3.3 Velocity Contour

The velocity contour generated from the CFD simulation delivers a comprehensive visualization of airflow behavior around the simplified Cybertruck model. At the front bumper, a pronounced stagnation region appears—signified by deep blue in the contour plot—where airflow velocity falls to nearly zero upon first impact with the almost vertical panel. This stagnation zone is characteristic of bluff-body aerodynamics, where abrupt geometry leads to sudden deceleration and localized pressure buildup [17]. Along the side panels, velocity increases as airflow accelerates to circumvent the bluff form. This acceleration is similar to the Venturi effect, as the color transitions from blue to green and yellow gradients in the contour. However, due to the sharp edges and angular geometry, airflow remains attached only briefly before separating [18].

At the rear, a substantial wake region forms, depicted by extensive low-velocity zones and irregular contour patterns. The sudden termination of the model's rear promotes early flow separation and prevents reattachment, resulting in persistent turbulence and recirculation zones.

These features exacerbate pressure drag, as the low-pressure region behind the vehicle generates a suction force opposing forward motion. Such behavior is typical in non-streamlined bluff-body configurations [19].

Moreover, the lack of rear tapering or curvature inhibits pressure recovery, thus maintaining high drag conditions. The observed wake size and intensity are consistent with prior CFD studies on simplified bluff bodies, emphasizing poor aerodynamic efficiency resulting from non-optimized geometries.

Figure 2 illustrates the velocity contour around the simplified Cybertruck model, highlighting the prominent stagnation zone at the front and the extensive wake structure behind the vehicle, consistent with aerodynamic attributes known to increase drag in bluff-body designs.

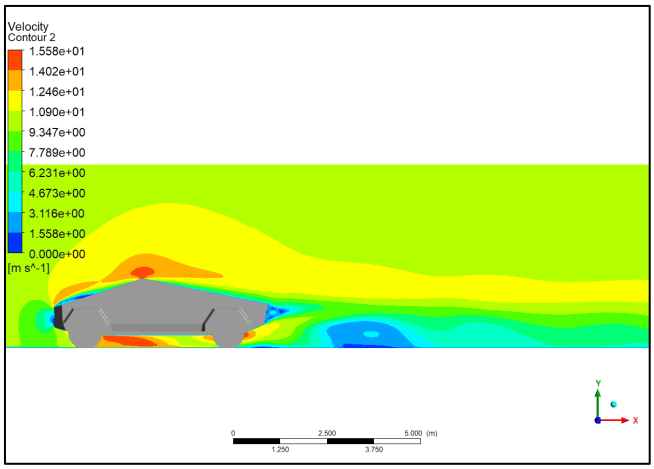

Fig. 2. Simulation Velocity Contour

3.4 Pressure Contour

The CFD simulation's static pressure contour reveals the bluff-body aerodynamics' pressure distribution characteristic around the Cybertruck model. At the front surface, a high-pressure region is evident, indicated by red and orange tones, forming a pronounced stagnation point where airflow decelerates to zero upon impact with the flat, vertical front panel. This abrupt deceleration leads to peak static pressure and contributes significantly to pressure drag—an effect well-documented in bluff-body flows [20]. Pressure decreases along the roof and side surfaces as the airflow accelerates, transitioning from yellow to green and blue in the contour plot. According to Bernoulli's principle, this pressure drop corresponds with increased velocity. However, the sharp edges of the Cybertruck geometry cause early boundary-layer separation, limiting effective pressure recovery on the vehicle's rear surfaces [21].

Behind the vehicle, the contour reveals a large low-pressure wake region, shown in dark blue. This extended wake results from flow separation at the abrupt rear end, which lacks taper or curvature. The resulting recirculation zones dramatically lower static pressure, increasing drag via a suction effect—a phenomenon consistent with non-streamlined bluff-body designs [22]. This pressure field distribution indicates that pressure drag dominates the overall aerodynamic profile of this geometry. The significant pressure differential between the front stagnation zone and rear wake highlights the importance of rear-end design features—such as boat-tail extensions or underbody diffusers—to recover pressure, reduce wake size, and improve aerodynamic efficiency [23].

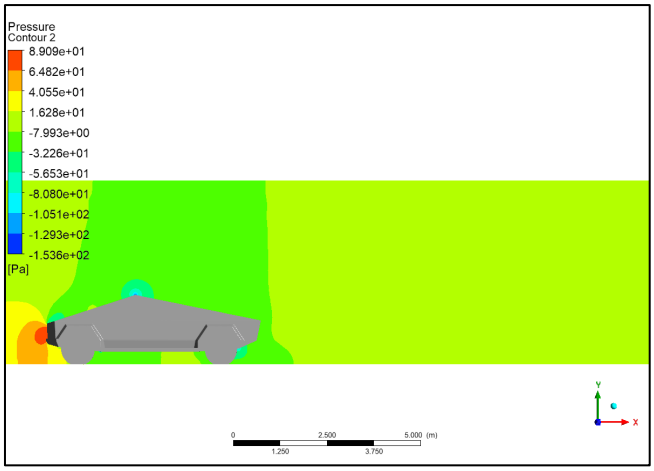

Fig. 3. Simulation pressure contour

3.5 Streamline

The streamline visualization generated through CFD simulation provides critical insights into the airflow behavior around the Cybertruck's bluff-body configuration. The streamlines approaching the vehicle's front exhibit a distinct deflection upon impacting the vertical surface, forming a stagnation zone where the airflow velocity drops to near zero. This region is characterized by high static pressure, consistent with classic bluff-body aerodynamics, where sharp front edges cause abrupt flow deceleration [24].

Moving along the sloped roofline, the streamlines accelerate and adhere to the surface momentarily, producing a low-pressure region above the windshield and roof, as evidenced by the curvature and color gradients transitioning from green to yellow. This acceleration follows Bernoulli's principle and demonstrates the limited curvature-induced flow attachment commonly observed in vehicles with sharp geometries [25].

Streamlining detachment becomes prominent in the rear half of the vehicle, particularly near the upper trailing edge. The lack of tapering and rear-end curvature leads to early separation and the formation of a turbulent wake, which is visible in the disorganized and diverging streamlines trailing the vehicle. This wake contributes significantly to pressure drag and aerodynamic inefficiency [26].

Additionally, flow separation is evident along the rocker panels and behind the front wheels, indicating vortex generation in the near-wake region. The disordered underbody streamlines also reflect the absence of aerodynamic enhancements such as diffusers or undertrays, essential for reducing ground-effect losses and improving streamline coherence [27].

The overall flow field depicted in the streamline plots confirms that the Cybertruck's sharp-edged, non-streamlined shape results in substantial wake formation and elevated pressure drag. This agrees with prior CFD studies on similar polygonal vehicle geometries, emphasizing the aerodynamic benefits of design refinements such as rear diffusers, chamfered edges, and tapering surfaces to improve flow attachment and reduce drag [27].

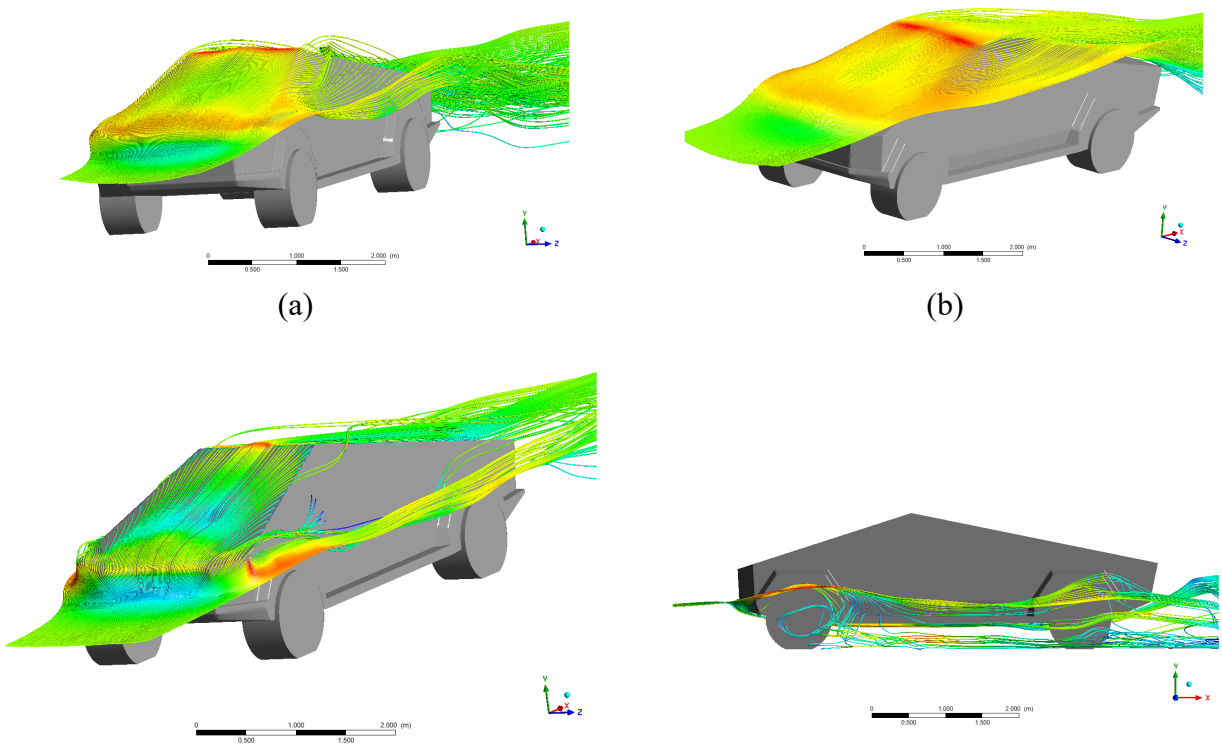

Fig. 4. (a) Front streamlines, (b) Top view, (c) Side view, (d) Rear underbody flow

3.6 Implications for Vehicle Efficiency

As speed increases, aerodynamic drag becomes the primary resistive force affecting vehicle motion, especially in electric vehicles, where it directly impacts energy consumption and driving range. Since drag force grows quadratically with speed, and power demand increases cubically, reducing the drag coefficient (Cd) is essential for improving efficiency.

Aerodynamic features such as tapered rears, smooth underbodies, and diffusers help reduce flow separation and wake formation, thus lowering drag. CFD enables early evaluation of these design strategies without costly prototypes, supporting more efficient and streamlined EV development.

4. Conclusions

This study presented an aerodynamic analysis of the Tesla Cybertruck using Computational Fluid Dynamics (CFD) simulations. The main objective was to evaluate how the vehicle's geometric shape influences drag coefficient, pressure distribution, flow behavior, and overall aerodynamic efficiency.

The simulation yielded a relatively high drag coefficient (Cd = 0.8418811), significantly above the typical range for electric vehicles. This result is attributed to the Cybertruck's flat surfaces and sharp edges, which induce early flow separation and generate a large wake behind the car. Pressure and velocity contours showed high-pressure buildup at the front and a large low-pressure wake at the rear, contributing substantially to pressure drag. The calculated drag force (Fd) and power requirement demonstrated a steep increase with velocity, underscoring the impact of aerodynamic drag on vehicle performance.

It is important to note that the model used in this study was a simplified representation of the actual Cybertruck, omitting detailed features such as underbody components, accessories, and surface curvature. These simplifications were made to reduce meshing complexity and computational cost, but may have affected the absolute accuracy of the drag coefficient. Therefore, the simulation results should be interpreted as indicative trends rather than exact predictions.

In summary, while the Cybertruck's unique shape contributes to distinctive aesthetics and structural strength, it also produces substantial aerodynamic penalties. Design improvements—such as rear tapering, diffusers, or underbody streamlining—may be necessary to reduce drag and enhance energy efficiency. Future research is encouraged to incorporate wind tunnel validation and more detailed geometries to refine and validate CFD-based findings.

Acknowledgement

The author would like to express sincere gratitude to the academic supervisors and faculty members who provided invaluable guidance and support throughout the development of this study. Appreciation is also extended to the institution's laboratory and computational facilities, which enabled the execution of the CFD simulations. Thanks to peers and colleagues who contributed constructive feedback during the simulation and documentation phases. Lastly, the author acknowledges the use of publicly available data and technical resources that were instrumental in modeling the simplified Cybertruck geometry for this research.

References

[1] Chongxu Wang dan Zitong Zhang. "The Aerodynamic Optimization of New Energy Vehicles." *Highlights in Science, Engineering and Technology*, Vol. 96 (2024): **29–39**. https://doi.org/10.54097/jmzwas23 -

[2] Xia, Zhijie, and Mengjun Huang. "Optimizing the Aerodynamic Efficiency of Electric Vehicles via Streamlined Design: A Computational Fluid Dynamics Approach." *International Journal of Heat & Technology* 42, no. 3 (2024). https://doi.org/10.18280/ijht.420315 -

[3] Paramasivan, Shankarsana. "Analysis of Tesla CyberTruck Speed on the Velocity and Pressure Distribution Using SimFlow Software." *Advanced and Sustainable Technologies (ASET)* 3, no. 1 (2024): 71-79.https://doi.org/10.58915/aset.v3i1.802 -

[4] Afianto, Darryl, Yu Han, Peiliang Yan, Yan Yang, Anas FA Elbarghthi, and Chuang Wen. "Optimisation and efficiency improvement of electric vehicles using computational fluid dynamics modelling." *Entropy* 24, no. 11 (2022): 1584. https://doi.org/10.3390/e24111584 -

[5] Valencia, Alvaro, and Nicolas Lepin. "Effect of Spoilers and Diffusers on the Aerodynamics of a Sedan Automobile." *International Journal of Heat & Technology* 42, no. 4 (2024). https://doi.org/10.18280/ijht.420406. -

[6] Badu, Prajash, Rahul Panjiyar, Kushal Guragain, and Pankaj Yadav. "CFD Analysis of Rear Spoiler Effects on Vehicles Aerodynamic Performance." *OODBODHAN* 7 (2024): 16-22.https://doi.org/10.3126/oodbodhan.v7i1.75760. -

[7] Buscariolo, Filipe F., Gustavo RS Assi, and Spencer J. Sherwin. "Computational study on an Ahmed Body equipped with simplified underbody diffuser." *Journal of Wind Engineering and Industrial Aerodynamics* 209 (2021): 104411.https://doi.org/10.1016/j.jweia.2020.104411. -

[8] Huminic, Angel, and Gabriela Huminic. "Aerodynamics of curved underbody diffusers using CFD." *Journal of Wind Engineering and Industrial Aerodynamics* 205 (2020): 104300. https://doi.org/10.1016/j.jweia.2020.104300. –

[9] Park, Gwanyong, Changmin Kim, Minhyung Lee, and Changho Choi. "Building geometry simplification for improving mesh quality of numerical analysis model." *Applied Sciences* 10, no. 16 (2020): 5425.https://doi.org/10.3390/app10165425

[10] Xu, Fusuo, Jianzhi Yang, and Xiaowei Zhu. "A comparative study on the difference of CFD simulations based on a simplified geometry and a more refined BIM based geometry." *Aip Advances* 10, no. 12 (2020). https://doi.org/10.1063/5.0031907

[11] Fu, Chen, Mesbah Uddin, and Chunhui Zhang. "Computational analyses of the effects of wind tunnel ground simulation and blockage ratio on the aerodynamic prediction of flow over a passenger vehicle." *Vehicles* 2, no. 2 (2020): 318-341. https://doi.org/10.3390/vehicles2020018

[12] Wang, Shibo, Terence Avadiar, Mark C. Thompson, and David Burton. "Effect of moving ground on the aerodynamics of a generic automotive model: The DrivAer-Estate." *Journal of Wind Engineering and Industrial Aerodynamics* 195 (2019): 104000.https://doi.org/10.1016/j.jweia.2019.104000

[13] Marcon, Julian, Michael Turner, Joaquim Peiro, David Moxey, Claire Pollard, Henry Bucklow, and Mark Gammon. "High-order curvilinear hybrid mesh generation for CFD simulations." In *2018 AIAA Aerospace Sciences Meeting*, p. 1403. 2018. https://doi.org/10.1016/j.cpc.2019.01.015

[14] Muflikhun, Muhammad Akhsin, Hifni Muktar Ariyadi, and Alfian Muhammad Fadhillah Hidayat. "The Evaluation of Mesh Characteristics of the Car Modeling and Simulation Using CFD Analysis." *Jurnal Rekayasa Mesin* 13, no. 1 (2022): 129-140. https://doi.org/10.21776/ub.jrm.2022.013.01.14

[15] Al-Saadi, Ahmed, Khaled Al-Farhany, Kadhim K. Idan Al-Chlaihawi, Wasim Jamshed, Mohamed R. Eid, El Sayed M. Tag El Din, and Zehba Raizah. "Improvement of the aerodynamic behavior of a sport utility vehicle numerically by using some modifications and aerodynamic devices." *Scientific Reports* 12, no. 1 (2022): 20272. https://doi.org/10.1038/s41598-022-24328-w

[16] Lintermann, Andreas. "Computational meshing for CFD simulations." In *Clinical and biomedical engineering in the human nose: A computational fluid dynamics approach*, pp. 85-115. Singapore: Springer Singapore, 2020. https://doi.org/10.1007/978-981-15-6716-2_6

[17] Guerrero, Alex, Robert Castilla, and Giorgio Eid. "A numerical aerodynamic analysis on the effect of rear underbody diffusers on road cars." *Applied Sciences* 12, no. 8 (2022): 3763. https://doi.org/10.3390/app12083763

[18] Rao, Anirudh N., Jie Zhang, Guglielmo Minelli, Branislav Basara, and Siniša Krajnović. "An LES investigation of the near-wake flow topology of a simplified heavy vehicle." *Flow, Turbulence and Combustion* 102, no. 2 (2019): 389-415.https://doi.org/10.1007/s10494-018-9959-6

[19] Pátý, Marek, Michael Valášek, Emanuele Resta, Roberto Marsilio, and Michele Ferlauto. "Passive Control of Vortices in the Wake of a Bluff Body." *Fluids* 9, no. 6 (2024): 131. https://doi.org/10.3390/fluids9060131

[20] Nebot, Eugeni Pérez, Antim Gupta, and Mahak Mahak. "Investigating the Impact of Structural Features on F1 Car Diffuser Performance Using Computational Fluid Dynamics (CFD)." *Mathematics* 13, no. 9 (2025): 1455. https://doi.org/10.3390/math13091455

[21] Moghimi, P., and R. Rafee. "Numerical and experimental investigations on aerodynamic behavior of the Ahmed body model with different diffuser angles." *Journal of Applied Fluid Mechanics* 11, no. 4 (2018): 1101-1113. https://doi.org/10.29252/jafm.11.04.27923

[22] Podvin, Bérengère, Stéphanie Pellerin, Yann Fraigneau, Antoine Evrard, and Olivier Cadot. "Proper orthogonal decomposition analysis and modelling of the wake deviation behind a squareback Ahmed body." *Physical Review Fluids* 5,no.6(2020):064612. https://doi.org/10.48550/arXiv.1909.13129

[23] Zhou, Haichao, Qingyun Chen, Runzhi Qin, Lingxin Zhang, and Huiyun Li. "Investigation of wheelhouse shapes on the aerodynamic characteristics of a generic car model." *Advances in Mechanical Engineering* 13, no. 12 (2021): 16878140211066842.doi: https://doi.org/10.1177/16878140211066842

[24] Aulakh, Deepinder Jot Singh. "Effect of underbody diffuser on the aerodynamic drag of vehicles in convoy." *Cogent Engineering* 3, no. 1 (2016): 1230310. doi: https://doi.org/10.1080/23311916.2016.1230310

[25] Ashton, Neil, Danielle C. Maddix, Samuel Gundry, and Parisa M. Shabestari. "AhmedML: High-fidelity computational fluid dynamics dataset for incompressible, low-speed bluff body aerodynamics." *arXiv preprint arXiv:2407.20801* (2024).https://doi.org/10.48550/arXiv.2407.20801

[26] Yuan, Zhiqun, Zhengqi Gu, Yiping Wang, and Xiaoqun Huang. "Numerical investigation for the influence of the car underbody on aerodynamic force and flow structure evolution in crosswind." *Advances in Mechanical Engineering* 10, no. 10 (2018): 1687814018797506. https://doi.org/10.1177/1687814018797506

[27] Alkan, B. (2020). *Aerodynamic Analysis of Rear Diffusers for a Passenger Car Using CFD*. OSF Preprints. https://doi.org/10.31224/osf.io/ntkq4